Chinese Journal of Natural Medicines

Shionone protects cerebral ischemic injury through alleviating microglia-mediated neuroinflammation

Lushan Xu, Chenggang Li, ChenChen Zhao, Zibu Wang, Zhi Zhang, Xin Shu, Xiang Cao, Shengnan Xia, Xinyu Bao, Pengfei Shao, Yun Xu

Citation: Lushan Xu, Chenggang Li, ChenChen Zhao, Zibu Wang, Zhi Zhang, Xin Shu, Xiang Cao, Shengnan Xia, Xinyu Bao, Pengfei Shao, Yun Xu, Shionone protects cerebral ischemic injury through alleviating microglia-mediated neuroinflammation, Chinese Journal of Natural Medicines, 2025, 23(4), 471-479. doi: 10.1016/S1875-5364(25)60812-0.

View online: https://doi.org/10.1016/S1875-5364(25)60812-0

Chinese Journal of Natural Medicines 23 (2025) 471-479

Contents lists available at ScienceDirect

Chinese Journal of Natural Medicines

journal homepage: www.cjnmcpu.com/

Original article

Shionone protects cerebral ischemic injury through alleviating microglia-mediated neuroinflammation

Lushan Xu[a,Δ], Chenggang Li[b,Δ], ChenChen Zhao[a,c], Zibu Wang[a,c], Zhi Zhang[a,c], Xin Shu[a,c], Xiang Cao[d,e], Shengnan Xia[c,d], Xinyu Bao[c,d], Pengfei Shao[c,d], Yun Xu[a,b,c,d,e,*]

[a] *Department of Neurology, Nanjing Drum Tower Hospital Clinical College of Nanjing University of Chinese Medicine, Nanjing 210008, China*
[b] *School of Pharmacy, Faculty of Medicine, Macau University of Science and Technology, Macau 999078, China*
[c] *Department of Neurology, Drum Tower Hospital, Medical School and The State Key Laboratory of Pharmaceutical Biotechnology, Institute of Translational Medicine for Brain Critical Diseases, Nanjing University, Nanjing 210008, China*
[d] *Jiangsu Key Laboratory for Molecular Medicine, Medical School of Nanjing University, Nanjing 210008, China*
[e] *Jiangsu Provincial Key Discipline of Neurology, Nanjing 210008, China*

ARTICLE INFO

Article history:
Received 11 November 2024
Revised 15 March 2025
Accepted 3 April 2025
Available online 20 April 2025

Keywords:
Shionone
Ischemic Stroke
Neuroinflammation
Microglial Activation
AKT-mTOR-STAT3 Signaling Pathway

ABSTRACT

Microglia, the resident immune cells in the central nervous system (CNS), rapidly transition from a resting to an active state in the acute phase of ischemic brain injury. This active state mediates a pro-inflammatory response that can exacerbate the injury. Targeting the pro-inflammatory response of microglia in the semi-dark band during this acute phase may effectively reduce brain injury. Shionone (SH), an active ingredient extracted from the dried roots and rhizomes of the genus *Aster* (Asteraceae), has been reported to regulate the inflammatory response of macrophages in sepsis-induced acute lung injury. However, its function in post-stroke neuroinflammation, particularly microglia-mediated neuroinflammation, remains uninvestigated. This study found that SH significantly inhibited lipopolysaccharide (LPS)-induced elevation of inflammatory cytokines, including interleukin-1β (IL-1β), tumor necrosis factor-α (TNF-α), and inducible nitric oxide synthase (iNOS), in microglia in *vitro*. Furthermore, the results demonstrated that SH alleviated infarct volume and improved behavioral performance in middle cerebral artery occlusion (MCAO) mice, which may be attributed to the inhibition of the microglial inflammatory response induced by SH treatment. Mechanistically, SH potently inhibited the phosphorylation of serine-threonine protein kinase B (AKT), mammalian target of rapamycin (mTOR), and signal transducer and activator of transcription 3 (STAT3). These findings suggest that SH may be a potential therapeutic agent for relieving ischemic stroke (IS) by alleviating microglia-associated neuroinflammation.

1. Introduction

Ischemic stroke (IS) accounts for 80% of all strokes and is associated with high morbidity, mortality, and disability rates [1]. Thrombolytic therapy remains the most effective treatment for IS, yet it is constrained by an exceedingly narrow therapeutic time window of 4 to 6 h after stroke onset [2]. Despite recent progress in stroke research, certain limitations and deficiencies persist with existing drug therapies [3]. Consequently, there is a pressing need to explore new, safe, and effective pharmacological interventions for the treatment of IS.

Neuroinflammation response, particularly that mediated by microglia, is essential for the pathological progression of IS in the early stage [4]. Microglia are the resident immune cells of the brain, responsible for maintaining central nervous system (CNS) homeostasis and modulating innate immune responses. In physiological conditions, microglia typically exhibit a small, ramified morphology, known as the "resting microglia" state. The disruption of brain homeostasis caused by IS leads to microglia activation, characterized by the thickening of dendritic branches and hypertrophy of the cell body [5]. Overactivated microglia exhibit a pro-inflammatory phenotype, producing an abundance of pro-inflammatory factors [6], such as interleukin-1β (IL-1β), tumor necrosis factor-α (TNF-α), and nitric oxide (NO), which exert toxic effects on neurons and subsequently exacerbate nerve tissue damage [7]. For instance, TNF-α plays a crucial role in glutamate excitotoxicity by blocking glutamate transporters on astrocytes and increasing the surface expression of AMPA receptors at glutamatergic synapses [8]. Furthermore, rapamycin has been reported to reduce neurodegeneration and decrease IL-1β and TNF-α production by inhibiting the mammalian target of rapamycin (mTOR) [9]. Therefore, suppressing microglia-associated neuroinflammation has become one of the therapeutic strategies for cerebral ischemia [10].

The serine-threonine protein kinase B (AKT), mTOR, and signal transducer and activator of transcription 3 (STAT3) signaling pathway is recognized as a critical component in various inflammatory conditions, including dermal inflammation [11] and trau-

* Corresponding author.
E-mail address: xuyun20042001@aliyun.com
Δ These authors contributed equally to this work.

https://doi.org/10.1016/S1875-5364(25)60812-0

matic brain injury-induced acute lung injury [12]. Recent research has demonstrated that heightened activation of the AKT-mTOR-STAT3 pathway within microglia plays a significant role in the exacerbation of IS [13]. Furthermore, downregulation of the AKT-mTOR-STAT3 signaling pathway has been shown to suppress the pro-inflammatory microglial phenotype and mitigate neuronal death [14].

Shionone (SH), a bioactive triterpenoid isolated from the dried roots and rhizomes of the *Aster* plant, family and rhizomes of the genus Aster (Asteraceae), is distributed in eastern Asia. Previous studies have indicated that it exerts anti-inflammatory effects on various inflammatory disease models, including attenuating lipopolysaccharide (LPS)-induced inflammation in RAW264.7 cells [15, 16] and alleviating sepsis-induced acute lung injury in mice through the ECM1/STAT5/NF-κB pathway [16]. In this study, we hypothesized that SH may have the potential to relieve microglial inflammation and potentially offer beneficial effects in the context of neurological injury following IS. To examine this conjecture, we investigated the effect and underlying mechanism of SH on microglia both *in vitro* and *in vivo* in the setting of IS, with the aim of identifying a novel therapeutic approach for this condition.

2. Materials and Methods

2.1. Cell culture

Primary microglia were prepared from the cortex of C57BL/6J mice [17], cultured in a humidified incubator at 37 °C for 10 days, and then shaken culture flasks to separate microglia, which were then re-implanted in 6-well or 12-well plates for 24 h after cell counting. The purity of microglia detected using the Iba1 antibody exceeded 95%. The cell culture conditions utilized Dulbecco's Modified Eagle Medium (DMEM, Thermo Fisher, USA) medium containing 10% fetal bovine serum (FBS, Biological Industries, Israel), 100 μg·mL^{-1} streptomycin, and 100 U·mL^{-1} penicillin.

Cortical neurons were isolated from E15-17 C57BL/6J mouse embryos. They were cultured and maintained in B27/neurobasal medium supplemented with glutamine for 10 days.

2.2. Treatment of microglia

In vitro experiments utilized LPS purchased from ALADDIN Ltd (Shanghai, China). SH (purity: ≥ 98%), obtained from MedChemExpress (Shanghai, China), was dissolved in ethanol, subjected to ultrasonication, and stored at −80 °C. SC79, an agonist of AKT, was acquired from MedChemExpress (Shanghai) and dissolved in dimethyl sulfoxide (DMSO). Primary microglia were divided into three groups based on equivalent density: control groups, LPS-only treatment groups, and drug-LPS treatment groups. Cells were pretreated with SH for 1 h and then exposed to LPS at a concentration of 100 ng·mL^{-1} for an additional 24 h. The concentration of DMSO did not exceed 0.1%.

2.3. Animals and middle cerebral artery occlusion (MCAO)

The study utilized healthy, male C57BL/6J mice aged approximately 8 weeks and weighing 20–25 grams, obtained from the Animal Model Center of Nanjing Medical University (Nanjing, China). All animal experiments were approved by the Animal Care and Use Committee of Nanjing University and conducted in accordance with institutional guidelines [18]. The experimental mice were housed in standard cages, maintained in a room with appropriate environmental conditions, and provided with adequate food and water.

Prior to establishing the MCAO model, 20 mice underwent behavioral training three days in advance, which included rotarod [19], paw grasping [20], and stepping rate assessments. To establish the MCAO mouse model, animals were anesthetized with avertin (2.5%), and a 6/0 monofilament nylon suture (Doccol Corporation, MA, USA) with a hot round tip was inserted through the internal carotid artery into the origin of the MCA until ipsilateral blood flow decreased to less than 30% of baseline values, as monitored using a laser Doppler flowmeter (Perimed Corporation, Sweden). The filaments were withdrawn after 60 min of occlusion to allow for blood reperfusion, and the mice were anesthetized and placed on a heating pad to maintain a temperature of 37 ± 0.5 °C until recovery [21]. Following the procedures, the mice were randomly divided into two groups: a saline-treated MCAO group (MCAO + Con) and a 20 mg·kg^{-1} SH-treated MCAO group (MCAO + SH). Over the next three days, the mice were provided adequate nutrition and care, and each mouse was intraperitoneally injected with pre-dissolved SH or the same volume of saline at 0.5, 24, and 48 h after MCAO induction [22].

2.4. Neuroscore assessment

Mice were evaluated for neurological function using the modified neurological severity score (mNSS) on the third day after MCAO. The mNSS, on a scale of 0 to 12, was utilized to measure motor, sensory, balance, and reflex function. The scores indicate the severity of brain damage. Neurological scores were evaluated in a single-blind manner for the experimental group [23]. Motor and sensorimotor functions were assessed through the rotarod test. Prior to establishing the MCAO model, mice underwent training on a rotarod device (RWD Life Science, China) twice daily for three consecutive days. The rotarod apparatus was set at speeds of 10, 20, 30, and 40 r·min^{-1} while accelerating the rotarod for 5–7 min at each speed, and the time each mouse ran on the rotarod was recorded at 40 r·min^{-1} on the third day. The footfault test is another behavioral test. The mice were trained twice a day for 5 min each time for three consecutive days. The wrong footstep of the left upper limb was recorded on the third day post-infarction. Additionally, the mouse paw grip strength was measured by a paw grip device for three days, and whether grip strength was affected was tested on the third day after MCAO [24].

2.5. Infarct volume measurement

At 72 h after MCAO, the mice underwent behavioral assessment. Subsequently, the brains of the model mice were rapidly removed, coronally sectioned into 1-mm-thick slices, and incubated with 2% 2,3,5-triphenyl tetrazolium chloride (TTC, Sigma-Aldrich, USA) solution for 10 min at 37 °C until the tissues were stained [25]. The infarct volume was analyzed using ImageJ (NIH, USA) software to calculate the infarct size across all brain layers. To mitigate the impact of brain edema, the ischemic hemisphere volume was calculated using the ipsilateral hemisphere volume as the baseline. The relative infarct volume is presented as the total infarct volume as a percentage of the whole brain volume.

2.6. Cell viability assays

As described, the microglia were cultured in a humidified incubator at 37 °C for 10 days. The microglial cells were then detached from the astrocytes by shaking the flasks, and the floating microglial cells were plated into 96-well plates at a density of 1 × 10^4 cells per well. The microglial cells were subsequently treated with varying concentrations of SH. After a 24-h incubation period, the viability of the microglia was assessed using the Cell Counting Kit-8 (CCK-8) kit (Dojindo Laboratories, Japan). The optical density (OD) of all wells was measured at 450 nm, and the cell viability was expressed as the percentage of the mean OD value of

the treated cells compared to the control group.

Additionally, the study combined neuronal medium with LPS and SH and added it to the microglia. After a 24-h incubation period, the supernatant was collected and added to the neurons overnight. The toxic impact of the microglial supernatant on neurons was further examined using the CCK-8 assay.

2.7. Western blotting analysis

Proteins were extracted from brain tissue in the ischemic penumbra and from microglia. The extracted proteins were separated using 10% sodium dodecyl sulfate (SDS)-polyacrylamide gel electrophoresis (PAGE) and transferred onto polyvinylidene fluoride (PVDF) membranes (Millipore, USA). The membranes were blocked with 5% skim milk for 2 h at room temperature and then cut horizontally according to different molecular weight levels. They were subsequently incubated with the appropriate primary antibodies, including *β*-tubulin (AP0064, Bioworld Biotechnology), anti-IL1-β (AB-401-NA, R&D Systems), anti-TNF-α (ab215188, Abcam), anti-iNOS/NOS (610328, BD Biosciences), phospho-AKT (p-AKT) (4060S, Cell Signaling Technology), phospho-STAT3 (p-STAT3) (9145S, Cell Signaling Technology), and phospho-mTOR (p-mTOR) (2971S, Cell Signaling Technology) overnight at 4 °C. Subsequently, the membranes were incubated with secondary antibodies for an additional 2 h at room temperature. Protein images were obtained using the Gel-Pro system (Tanon Technologies, China), and the quantification of the blot intensity was calculated using ImageJ. The p-AKT, p-STAT3, and p-mTOR antibodies were stripped using primary and secondary antibody removal solutions for 10 min and stripped only once. The membranes were then washed with TBST and coated with the corresponding non-phosphorylated antibodies, such as AKT (4685S, Cell Signaling Technology), STAT3 (9139S, Cell Signaling Technology), and mTOR (BS3611, Bioworld Biotechnology).

ImageJ software was utilized to analyze the grayscale values of the protein bands. The grayscale values of the target proteins were compared to the grayscale values of the corresponding internal control bands to determine protein expression levels, which represented the relative content of the target protein in the samples. Furthermore, changes in the ratio of phosphorylated protein to total protein were used to explain alterations in phosphorylation levels. Statistical and analytical analyses were conducted using GraphPad Prism 7.0.

2.8. Real-time polymerase chain reaction (PCR)

PCR primers were purchased from Tsingke Biotechnology Co, Ltd. Primary microglia were cultured with SH for 1 hour and stimulated with 0.1 μg·mL^{-1} LPS for 24 h. Infarcted tissue mRNA was extracted from mice on the third day after MCAO. Total mRNA was reverse transcribed into complementary DNA (cDNA) using the PrimeScript RT reagent kit (Vazyme, China) [26]. The expression of specific genes was analyzed on a LightCycler 96 PCR system (Roche, Switzerland) using an SYBR Green Kit (Vazyme, China). The primer sequences are provided below:

TNF-α: Forward, 5'- CAAGGGACAAGGCTGCCCCG-3'

The sequence 5'-GCAGGGGCTCTTGACGGCAG-3' serves as the reverse primer in this study.

IL1-β: Forward, 5'- AAGCCTCGTGCTGTCGGACC-3'

The reverse primer sequence is 5'-TGAGGCCCAAGGCCACAGG-3'.

Inos: Forward, 5'-CAGCTGGGCTGTACAAACCTT-3'

The sequence provided, 5'-CATTGGAAGTGAAGCGTTTCG-3', represents the reverse, or complementary, strand of a nucleic acid sequence.

Gapdh: Forward, 5'-GCCAAGGCTGTGGGCAAGGT-3'

Reverse primer, 5'-TCTCCAGGCGGCACGTCAGA-3'

Relative quantitative methods were utilized to analyze quantitative polymerase chain reaction (qPCR) data. The primary unit employed is fold change, calculated predominantly using the $2^{-\triangle\triangle Ct}$ method. This approach indicates the difference in expression of the target gene between the experimental and control groups.

2.9. Flow cytometry and microglia isolation

After inducing an MCAO model in mice, the infarcted hemispheres were collected, ground in a buffer solution containing 25% glucose and HEPES, and passed through a 70-μm filter to obtain a single-cell suspension. The cell suspension was then layered on a 30%−70% Percoll gradient and centrifuged to separate the cells. The top layer containing myelin was discarded, and the cells at the junctions were collected. These cells were then stained with antibodies against the microglial markers CD45, CD11b, and CD86 for analysis.

Primary microglia were subjected to flow cytometry analysis. The cells were first digested, washed twice with phosphate-buffered saline (PBS), and re-suspended in cold PBS at a density of 1×10^6 cells/mL. The microglia were then incubated with the following fluorescently-labeled antibodies in the dark at 4 °C for 30 min: CD45-PE/CY7 (Biolegend, 100422, 1∶500), CD11b-APC (eBioscience, 17-0112-82, 1∶500), and CD86-BV421 (BD Horizon, 564198, 1∶500). The expression of CD86 was subsequently detected using a FACS Calibur flow cytometer (BD Biosciences).

2.10. Immunofluorescence staining

Three days after MCAO, brain tissues were dehydrated and cut into 20 μm sections [27]. Microglia were fixed with 4% paraformaldehyde for 15 min. The slices and cells were washed three times with PBS, then the slices or primary microglia were permeated with 0.1% Triton X-100 for 10 min and blocked with 2% bovine serum albumin (BSA) for 90 min. Sections and microglia were incubated overnight at 4 °C with primary antibodies against ionized calcium-binding adapter molecule 1 (Iba1, 1∶500; Wako, Japan) or cluster of differentiation 86 (CD86, 1∶1000; Abcam, USA). These samples were then incubated with the indicated secondary antibodies for 2 h at room temperature in the dark. 4′,6-diamidino-2-phenylindole (DAPI, 10 μg·mL^{-1}, Beyotime) was added for 15 min to stain the nuclei. Images were obtained using an Olympus BX51 (Japan) fluorescence microscope, and the relative area and mean fluorescence intensity (MFI) of microglia were analyzed using ImageJ software (ImageJ 1.5, National Institutes of Health).

2.11. Enzyme-linked immunosorbent assay (ELISA)

The tissue of the cerebral infarction hemisphere was collected 3 days after MCAO. The tissue was ground and homogenized on ice, and the supernatant containing microglia was collected. The supernatant was centrifuged for 10 min to remove the cellular pellet. ELISAs were performed to determine the levels of IL-1β and TNF-α using commercial kits (Bioworld Biotechnology, USA) according to the manufacturer's instructions. The enzyme marker was used for dual-wavelength detection within 30 min, and the maximum absorption wavelength was measured at 450 nm. A standard curve was generated by plotting the standard concentration against the OD values, and the fitted equation was used to calculate the corresponding cytokine concentrations based on the OD values obtained from the samples.

2.12. Statistical analysis

The data results are expressed as the mean ± standard error of the mean (SEM) for the different experimental groups. The

statistical significance of differences between two groups was calculated using the Student's *t*-test, while the significance of differences among three or more groups was evaluated through one-way analysis of variance (ANOVA). *P*-values less than 0.05 were deemed statistically significant.

3. Results

3.1. SH reversed microglial morphological changes after LPS stimulation and its effect on microglial cell viability

To investigate the cytotoxic effects of SH (Fig. 1A) on microglia, primary cultured microglia were subjected to a CCK-8 viability assay after treatment with varying concentrations of SH (1, 5, 20, 40, 50, 100 μmol·L^{-1}) for 24 h. The results indicated that microglial viability remained unaffected at concentrations below 50 μmol·L^{-1} (Fig. 1B). Consequently, concentrations below 50 μmol·L^{-1} were selected for further research. After SH treatment, the morphological changes of microglia were evaluated, revealing that SH could gradually inhibit LPS-induced microglial enlargement (Figs. 1C and 1D) and attenuate Iba1 fluorescence intensity as the concentration increased (Figs. 1C and 1E). In addition, the results of the CCK8 test showed that SH could rescue the toxic effect of LPS-stimulated microglial supernatant on neurons (Fig. 1F). These findings suggest that SH can reverse the morphological changes and toxicity of LPS-induced microglia.

3.2. SH reduced LPS-induced pro-inflammatory cytokines in primary microglia

To assess the protective effect of SH on neuroinflammation, various pro-inflammatory cytokines were examined. The study demonstrated that pretreatment of primary microglia with SH could significantly reduce the mRNA (Figs. 2A–2C) and protein levels (Figs. 2E–2H) of IL-1β, TNF-α, and iNOS after LPS stimulation in a dose-dependent manner. Furthermore, we detected IL-1β and TNF-α expression respectively by ELISA *in vitro* experiments, and we found that IL-1β and TNF-α expression was decreased in the SH group (Figs. 2I–2J). Additionally, the MFI of CD86, a microglial inflammatory marker, was found to be higher in LPS-stimulated primary microglia by flow cytometry, while CD86 expression was reduced in SH-treated microglia (Figs. 2K and 2L). These results indicate that SH can inhibit the LPS-induced inflammatory response in primary microglia.

3.3. SH attenuates brain injury and neurological deficits after cerebral ischemia

The study then examined the impact of SH on IS *in vivo*. The

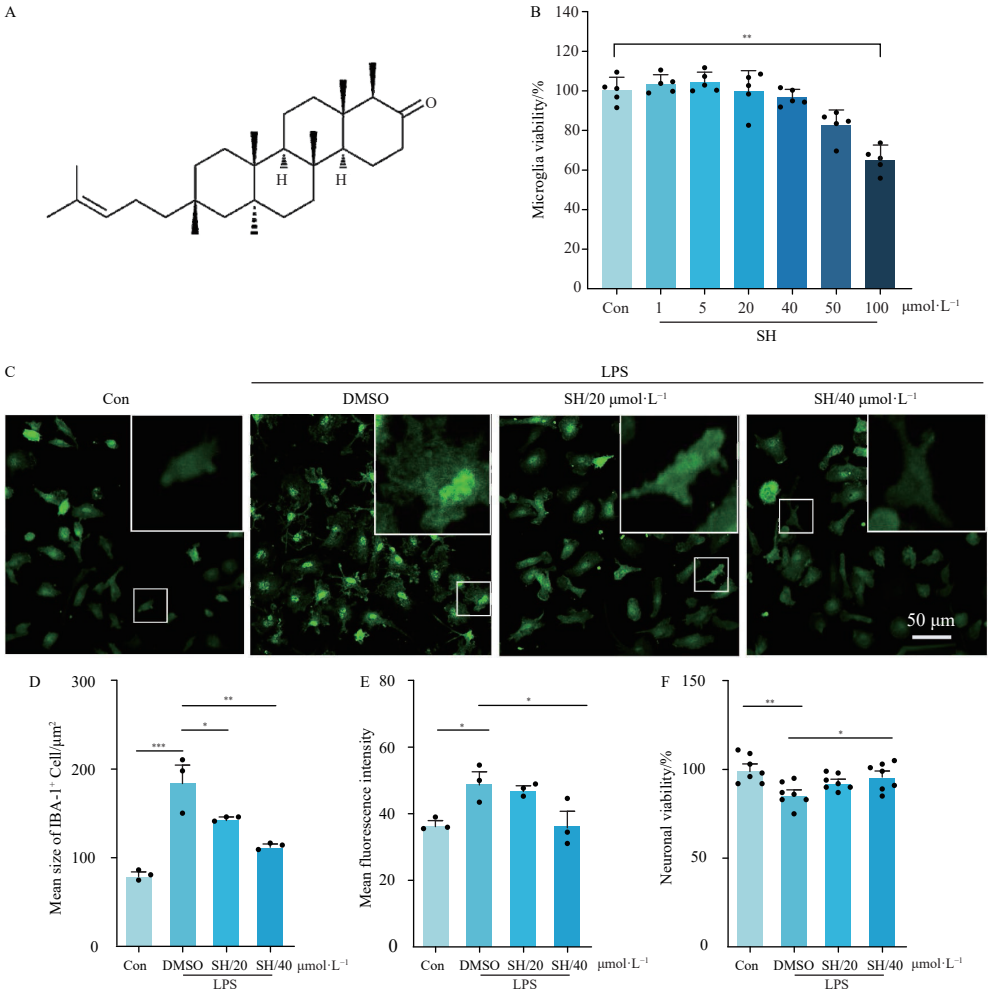

Fig. 1 SH reversed microglial morphological changes after LPS stimulation and its effect on microglial cell viability. (A) Chemical structure of SH. (B) Effects of SH on cell viability. Primary microglia were treated with different concentrations of SH (1, 5, 20, 40, 50, or 100 μmol·L^{-1}). After 24 h, the CCK-8 assay was used to evaluate cell viability. (C) Microglia were pretreated with various concentrations of SH (20, 40 μmol·L^{-1}) for 1 h, and then treated with 0.1 μg·mL^{-1} LPS for 24 h. The microglia were examined by immunocytochemical staining with Iba1 antibody (Bar = 50 μm). (D) The mean size of Iba1$^+$ cells (μm^2) and (E) MFI of Iba1 in (C) were measured by ImageJ. (F) Microglia were stimulated by diluting LPS and SH (20, 40 μmol·L^{-1}) with neuronal medium, and then neurons were treated with the supernatant of microglia for 24 h. Neuronal viability was measured by CCK-8 assay. Results are expressed as the mean of three independent experiments ± SEM (n = 3). $^*P < 0.05$; $^{**}P < 0.001$ and $^{***}P < 0.001$.

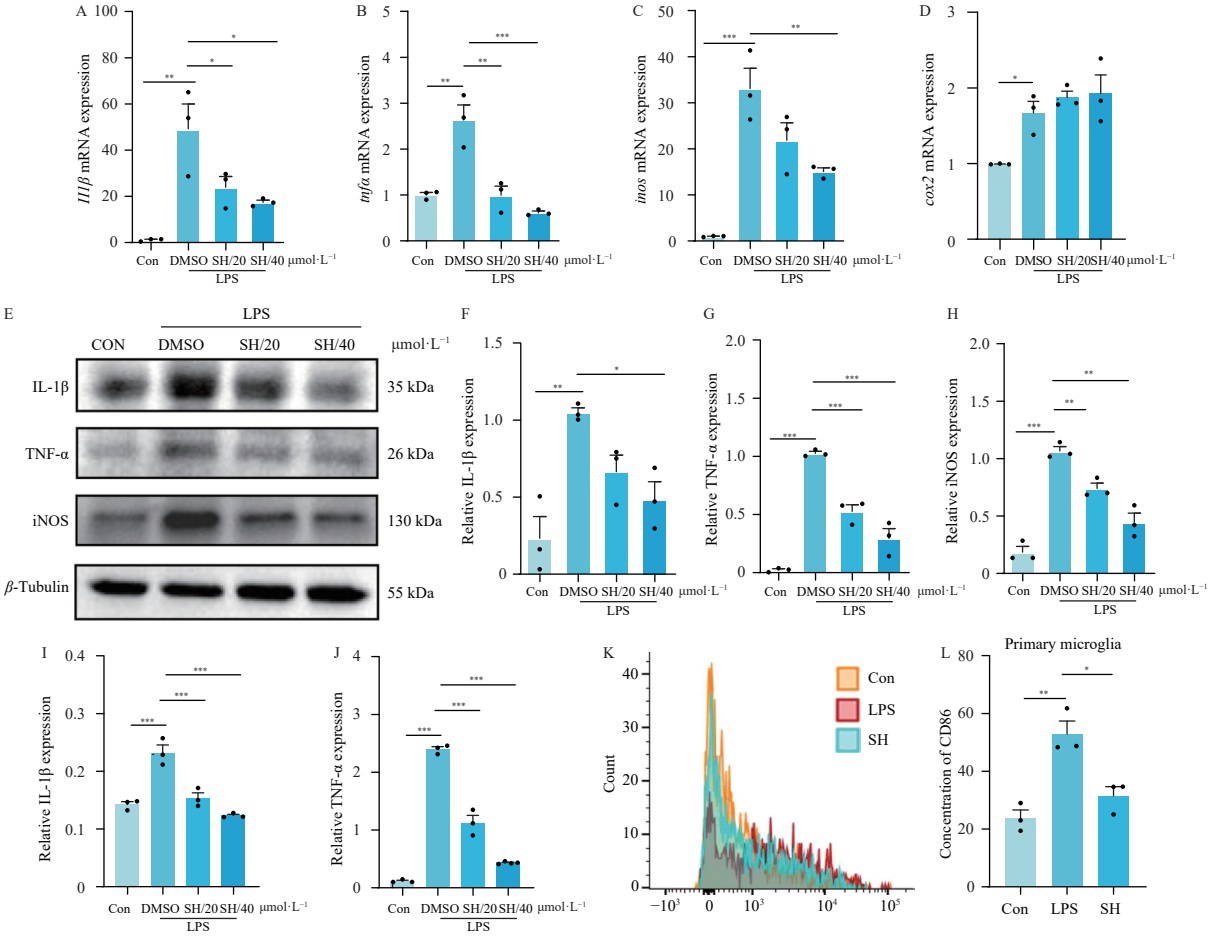

Fig. 2 Effect of SH on LPS-induced inflammatory cytokine production in primary microglia. Microglia were pretreated with different concentrations of SH (20, 40 μmol·L^{-1}) for 1 h and then treated with 0.1 μg·mL^{-1} LPS for 24 h. The expression levels of *Il1β* (A), *tnfα* (B), and *inos* (C), and *cox2* (D) mRNA were measured using real-time PCR. (E) The expression of IL-1β, TNF-α, and iNOS proteins was examined by western blotting, with *β*-tubulin as a loading control. Statistical results of IL-1β (F), TNF-α (G), and iNOS (H) protein expression levels were measured using ImageJ. Protein levels of IL-1β (I) and TNF-α (J) were also detected by ELISA. (K–L) Microglia were pretreated with 40 μmol·L^{-1} SH for 1 h and then treated with 0.1 μg·mL^{-1} LPS for 24 h. The effect of SH on the average fluorescence intensity of CD86 was detected by flow cytometry. The results are expressed as the mean ± SEM of three independent experiments. $^{*}P < 0.05$, $^{**}P < 0.01$, and $^{***}P < 0.001$.

findings demonstrated that the infarct volume of MCAO mice treated with SH for three days was significantly reduced compared to the control group, as measured by TTC staining (Figs. 3A and 3B). Furthermore, the cerebral ischemic mice suffered a better neurological function evaluation, including the mNSS test, paw grasping, rotary running, and the wrong stepping rate after SH treatment (Figs. 3C–3F). Collectively, these data indicated that SH attenuated brain injury and neurological deficits in cerebral ischemic mice.

3.4. SH reduced the activation of pro-inflammatory microglia in vivo

Immunofluorescence staining of CD86, a marker of pro-inflammatory microglia, demonstrated a reduction in fluorescence intensity of CD86 in microglia following SH treatment (Figs. 4A and 4B). Further analysis using flow cytometry revealed a decrease in the mean fluorescence intensity of CD86 in microglial cells of SH-treated mice (Figs. 4C and 4D). These findings indicate that SH can inhibit the activation of pro-inflammatory microglia in the MCAO mouse model.

3.5. SH suppressed the expression of inflammatory cytokines in vivo

This study examined the mRNA levels of *Il1b*, *tnfa*, and *inos* in the penumbra. The results indicated that these pro-inflammatory cytokines were significantly reduced in the SH-treated ischemic brain (Figs. 5A–5C). Further analysis by Western Blotting (Figs. 5D–5G) and ELISA (Fig. 5H–5I) demonstrated that SH could reverse the increase of IL-1β, TNF-α, and iNOS protein levels following MCAO. The consistent changes observed in the production and secretion of these pro-inflammatory cytokines at both the mRNA and protein levels suggest that SH can inhibit pro-inflammatory responses in the penumbra of the ischemic hemisphere.

3.6. SH exerted a protective effect through the AKT-mTOR-STAT3 signaling pathway

Next, we aimed to further explore the possible mechanism of SH in reducing microglial activation and the expression of inflammatory factors. We assessed primary microglia on the expression of AKT, mTOR, and STAT3 by using Western Blot and found that the phosphorylation of STAT3, AKT, and mTOR was significantly increased after LPS treatment, while SH decreased the phosphorylation of STAT3, AKT, and mTOR in LPS-treated microglia (Figs. 6A, 6C–6E). Additionally, the analysis of proteins extracted from the brain tissue in the penumbra of the ischemic hemisphere revealed that the phosphorylation of AKT, mTOR, and STAT3 was also significantly decreased *in vivo* compared to the control group (Figs. 6B, 6F–6H). To further investigate whether the AKT-mTOR-STAT3 pathway is associated with the anti-inflammatory effects of SH, we supplemented the LPS + SH + AKT agonist SC79 (4 μg·mL^{-1}) group [28]. As shown in the graphs (Figs. 6I–6K), the results revealed that the anti-inflammatory activity of SH disappeared after AKT activation, suggesting that SH specific-

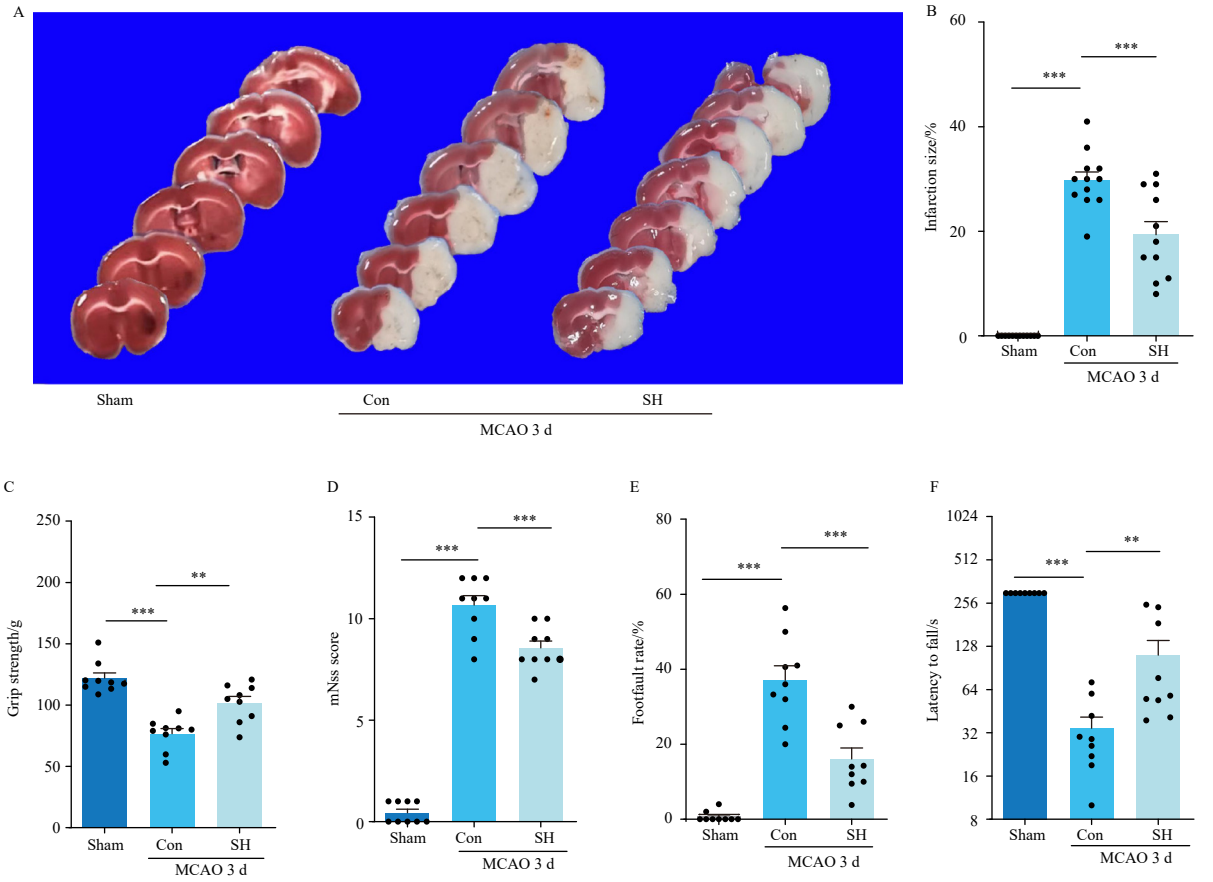

Fig. 3 SH alleviated brain injury and neurological deficits in mice three days after MCAO. Mice after MCAO were treated with drugs or saline for three consecutive days for behavioral testing. (A) TTC staining at 3 days after MCAO. (B) Infarct volume of each group (n = 10 per group). The results of (C) grip strength, (D) mNSS scores, (E) foot-fault test rate, and (F) latency to fall. The results were expressed as the mean ± SEM of three independent experiments. $^{*}P < 0.05$, $^{**}P < 0.01$, and $^{***}P < 0.001$.

ally inhibits lps-induced expression of microglial inflammatory factors through the AKT-mTOR-STAT3 signaling pathway.

4. Discussion

This study identified a novel anti-neuroinflammatory compound, SH. SH demonstrated the capacity to significantly reduce the expression of pro-inflammatory cytokines, including IL-1β, TNF-α, and inducible nitric oxide synthase (iNOS), in LPS-stimulated cultured microglia cells and the penumbra region of a MCAO mouse model. The anti-inflammatory effects of SH on the MCAO mouse model improved neurological behaviors and decreased infarct volume, consistent with the compound's ability to inhibit the LPS-induced inflammatory response in acute lung injury models using RAW264.7 cells [16]. These findings suggest that SH may serve as an effective neuroprotective agent with potential applications in the treatment of IS.

As resident cells of the brain, microglia contribute to the development and homeostasis of the CNS by supporting neuronal survival, apoptotic program, and synaptogenesis in the normal brain [29]. Typically, microglia exist in a resting state, exhibiting a highly branched morphology. However, when brain homeostasis is disrupted after stroke onset, microglia undergo rapid activation and transformation into an amoeboid shape, leading to the release of inflammatory factors, synaptic degeneration, nerve cell death, and neurotoxicity [30]. Iba1 is a 17-kDa EF-hand calcium-binding protein widely expressed in macrophages and microglia, and its levels are significantly elevated when these cells are activated [31]. In this research, after SH treatment, the morphology of microglia and the fluorescence intensities of Iba1 were reversed, indicating that SH suppressed microglial activation and thereby exerted a potential neuroprotective effect.

Following cerebral ischemia, microglia undergo a transformation into a pro-inflammatory phenotype, releasing inflammatory mediators such as TNF-α, IL-1β, NO, and interferon-γ (IFN-γ), accompanied by an increase in CD86 expression [32]. These pro-inflammatory cytokines, IL-1β and TNF-α, can exacerbate brain injury by activating damaging signaling pathways (e.g., NF-κB and JNK/AP-1), leading to blood-brain barrier disruption and the initiation of apoptotic mechanisms (such as glutamate-mediated excitotoxicity) [33-35]. Furthermore, iNOS interacts with other inflammatory factors, like IL-1β and TNF-α, and is involved in the inflammatory cascade [36]. Numerous studies have reported that the reduction of CD86, a pro-inflammatory microglial marker, inhibits its neuronal apoptosis in the brain[37]. Therefore, the synthesis, secretion, and biological activity of these pro-inflammatory cytokines represent potential therapeutic targets for IS. Our data indicate that SH inhibited the microglial expression of pro-inflammatory factors (such as IL-1β, TNF-α, and iNOS) and CD86 following IS, suggesting the neuroprotective effect of SH.

P-AKT is a major effector of the AKT-mTOR-STAT3 pathway, which regulates cellular functions by activating various transcription factors, kinases, and enzymes [38]. mTOR, a downstream target of p-AKT, is a serine-threonine protein kinase regulated by proline and is stimulated by various factors that mediate essential biological processes in the brain [39]. STAT proteins belong to a family of transcription factors that play an important role in cellular signal transduction. Similar to the mTOR protein, STAT3 integrates extracellular signals (like cytokines) from the interferon and interleukin families [40]. The AKT-mTOR-STAT3 pathway, which has been reported as a key signal transduction pathway in the inflammatory response, is highly activated in microglia after IS and is involved in the aggravation of disease damage [13]. The data presented here showed that the phosphorylation levels of

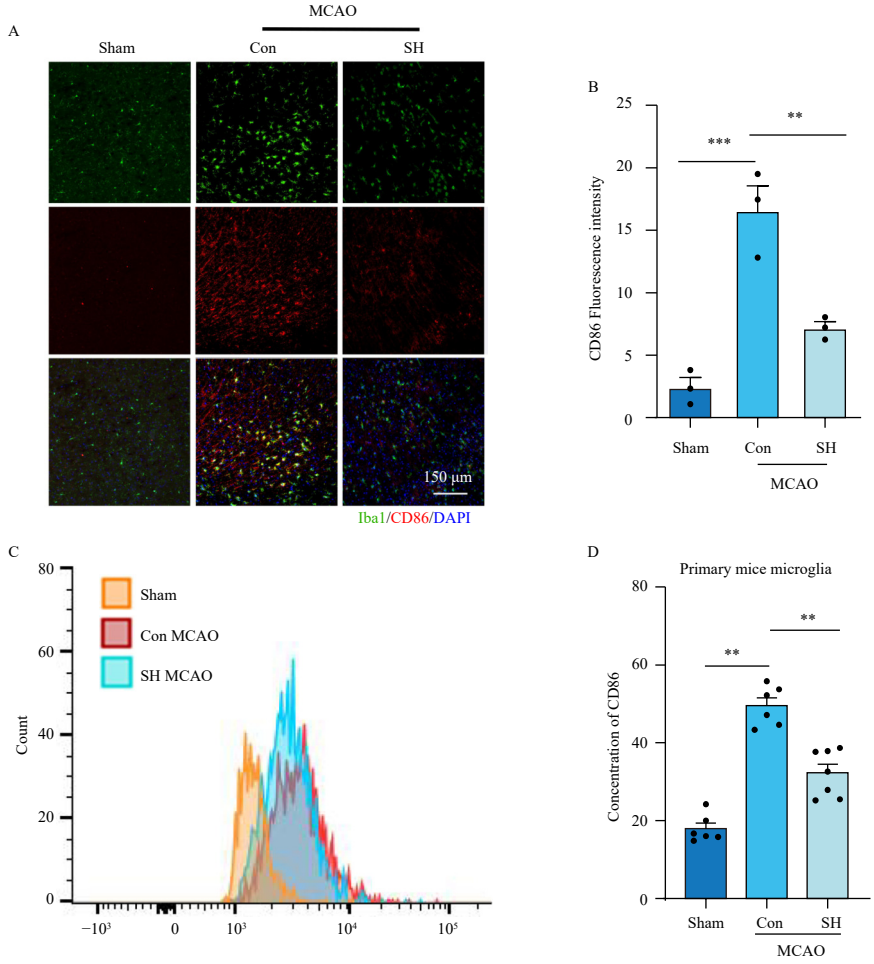

Fig. 4 SH reduced the activation of pro-inflammatory microglia *in vivo*. (A) Brain slices were analyzed by immunofluorescence using antibodies targeting Iba1 and CD86 (Scale bar = 150 μm). (B) The MFI of CD86 in Iba1-positive cells was measured using ImageJ. (C–D) The mean fluorescence intensity of CD86 in microglial cells of SH-treated mice was analyzed by flow cytometry. The results are expressed as the mean ± SEM of three independent experiments. $^{*}P < 0.05$, $^{**}P < 0.01$, and $^{***}P < 0.001$.

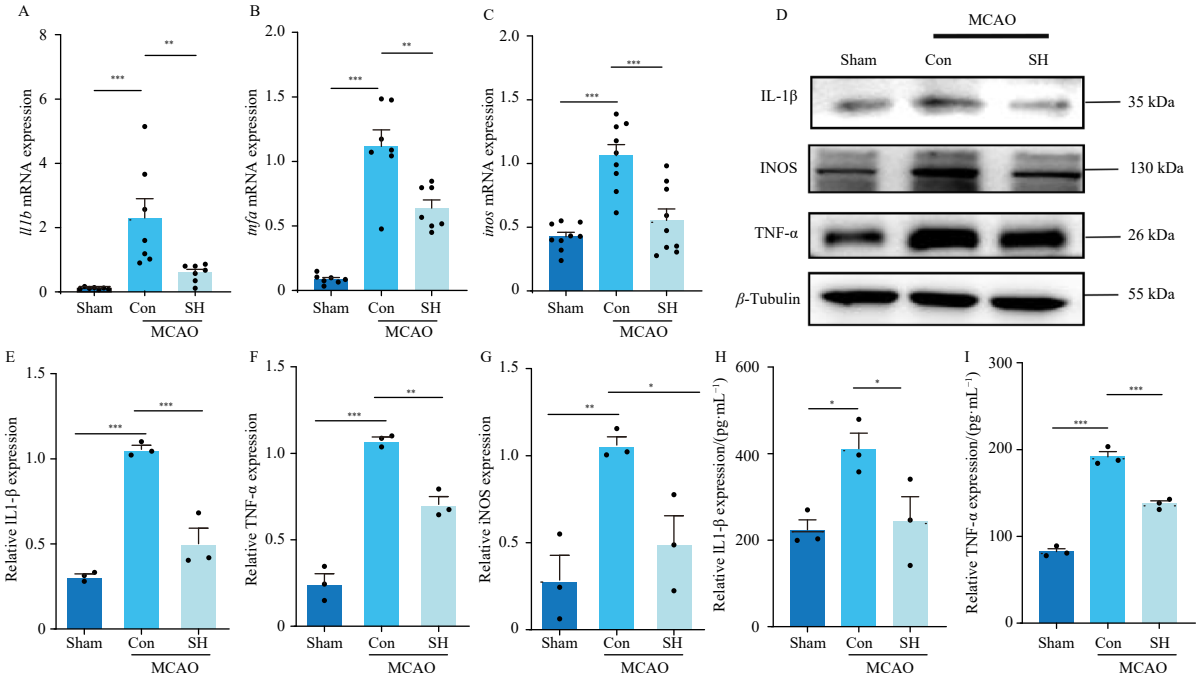

Fig. 5 SH suppressed the expression of inflammatory cytokines *in vivo*. Three days after MCAO, intraperitoneal injection of SH or saline was performed, and the mRNA expression of *Il1b* (A), *tnfa* (B), and *inos* (C) in the penumbra was assessed by real-time PCR ($n = 9$). (D) Western blotting with *β*-tubulin as a loading control was used to examine the expression of IL-1β, TNF-α, and iNOS proteins. The statistical results of IL-1β (E), TNF-α (F), and iNOS (G) protein expression levels were measured using ImageJ. Protein levels of IL-1β (H) and TNF-α (I) were also detected by ELISA. The results are expressed as the mean ± SEM of three independent experiments. $^{*}P < 0.05$, $^{**}P < 0.01$, and $^{***}P < 0.001$.

AKT, mTOR, and STAT3 were decreased after treatment with SH. Moreover, the highly selective AKT agonist SC79 [28] was used to validate the specific effect of SH on the AKT-mTOR-STAT3 pathway during neuroinflammation. As shown in the graphs (Figs. 6 I–6K), the anti-inflammatory activity of SH disappeared after AKT activation, suggesting that SH specifically inhibits LPS-induced expression of microglial inflammatory factors through the AKT-mTOR-STAT3 signaling pathway. These findings confirm that SH pretreatment inhibits the inflammatory response of activated microglia by modulating the AKT-mTOR-STAT3 pathway. Meanwhile, there was no significant change in microglial NF-κB and ERK phosphorylation levels in microglia after LPS stimulation (not shown), indicating that the anti-inflammatory effect of SH on microglia did not work through these pathways.

In summary, this study revealed the protective effects of SH against IS injury and its anti-inflammatory action on microglia and the potential underlying mechanism involving the inhibition of the AKT-mTOR-STAT3 signaling pathway. These findings indic-

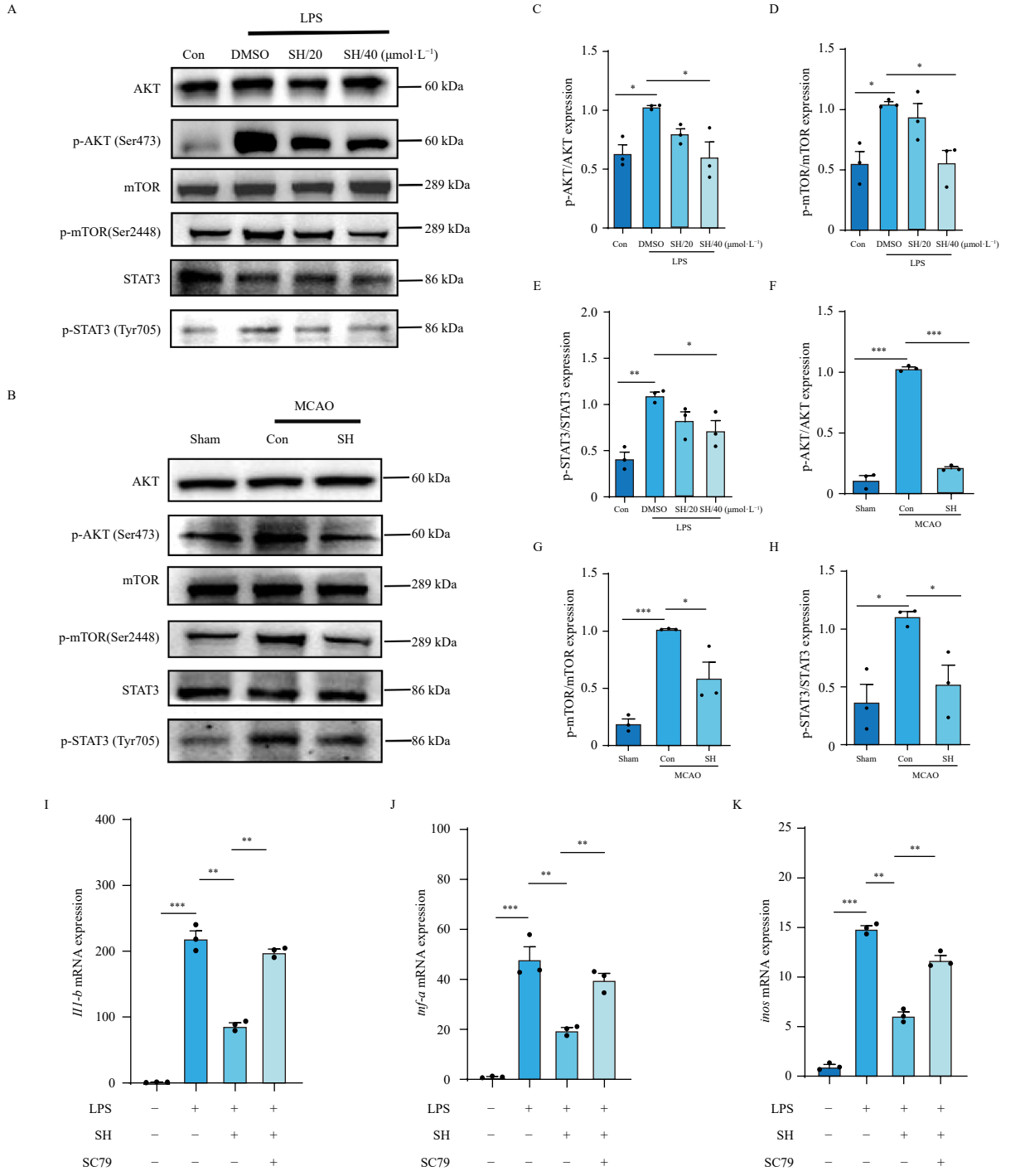

Fig. 6 SH inhibited the LPS-induced AKT-mTOR-STAT3 signaling pathway in microglia and the MCAO demonstrates that SH inhibited the LPS-induced AKT-mTOR-STAT3 signaling pathway in microglia and the MCAO mouse model. Microglia were pretreated with varying concentrations of SH (20, 40 μmol·L^{-1}) for 1 h and then exposed to 0.1 μg·mL^{-1} LPS for 0.5 h. The protein expression of AKT, STAT3, mTOR, and their corresponding phosphorylated forms (p-AKT, p-STAT3, p-mTOR) was analyzed by western blotting (A). The ratios of p-AKT/AKT (C), p-mTOR/mTOR (D), and p-STAT3/STAT3 (E) were quantified using ImageJ. In the MCAO mouse model, SH or saline was administered intraperitoneally 3 d after MCAO, and the expression of these proteins in the penumbra was detected by western blotting (B). The ratios of p-AKT/AKT (F), p-mTOR/mTOR (G), and p-STAT3/STAT3 (H) were also measured using ImageJ. Additionally, LPS-activated microglia were treated with the AKT agonist SC79 (4 μmol·L^{-1}), and the expression of *Il1b*, *tnfa*, and *inos* mRNA was assessed (I–K). The results are presented as mean ± SEM for three independent experiments. $^{*}P < 0.05$, $^{**}P < 0.01$, and $^{***}P < 0.001$.

ate that SH may offer a new therapeutic approach for the treatment of IS.

Funding

This work was supported by the National Natural Science Foundation of China (Nos. 81920108017 and 82130036), the Key Research and Development Program of Jiangsu Province of China (No. BE2020620), and Jiangsu Province Key Medical Discipline (No. ZDXKA2016020).

Declaration of Competing Interest

These authors have no conflict of interest to declare.

References

1 Phipps MS Cronin CA. Management of acute ischemic stroke. *BMJ*. 2020;368: l6983. https://doi.org/10.1097/CCM.0000000000004597.
2 Lambertsen KL, Finsen B, Clausen BH. Post-stroke inflammation-target or tool for therapy?. *Acta Neuropathol*. 2019;137(5):693-714. https://doi.org/10.1007/s00401-018-1930-z.
3 Deng SJ, Ge JW, Xia SN, et al. Fraxetin alleviates microglia-mediated neuroinflammation after ischemic stroke. *Ann Transl Med*. 2022;10(8):439. https://doi.org/10.21037/atm-21-4636.
4 Stoll G, Nieswandt B. Thrombo-inflammation in acute ischaemic stroke-implications for treatment. *Nat Rev Neurol*. 2019;15(8):473-481. https://doi.org/10.1038/s41582-019-0221-1.
5 Qin C, Zhou LQ, Ma XT, et al. Dual functions of microglia in ischemic stroke. *Neurosci Bull*. 2019;35(5):921-933. https://doi.org/10.1007/s12264-019-00388-3.
6 Xu L, He D, Bai Y. Microglia-mediated inflammation and neurodegenerative disease. *Mol Neurobiol*. 2016;53(10):6709-6715. https://doi.org/10.1007/s12035-015-9593-4.
7 Kim E, Cho S. Microglia and monocyte-derived macrophages in stroke. *Neurotherapeutics*. 2016;13(4):702-718. https://doi.org/10.1007/s13311-016-0463-1.
8 Pickering M, Cumiskey D, O'Connor JJ. Actions of TNF-α on glutamatergic synaptic transmission in the central nervous system. *Exp Physiol*. 2005;90(5): 663-670. https://doi.org/10.1113/expphysiol.2005.030734.
9 Yin L, Ye S, Chen Z, et al. Rapamycin preconditioning attenuates transient focal cerebral ischemia/reperfusion injury in mice. *Int J Neurosci*. 2012;122 (12):748-756. https://doi.org/10.3109/00207454.2012.721827.
10 Jin R, Yang G, Li G. Inflammatory mechanisms in ischemic stroke: role of inflammatory cells. *J Leukoc Biol*. 2010;87(5):779-789. https://doi.org/10.1189/jlb.1109766.
11 Cai Y, Xue F, Qin H, et al. Differential roles of the mTOR-STAT3 signaling in dermal γδ T cell effector function in skin inflammation. *Cell Rep*. 2019;27(10): 3034-3048 e3035. https://doi.org/10.1016/j.celrep.2019.05.019.
12 Xu X, Zhi T, Chao H, et al. ERK1/2/mTOR/Stat3 pathway-mediated autophagy alleviates traumatic brain injury-induced acute lung injury. *Biochim Biophys Acta Mol Basis Dis*. 2018;1864(5 Pt A):1663-1674. https://doi.org/10.1016/j.bbadis.2018.04.003.
13 Liu Y, Deng S, Zhang Z, et al. 6-Gingerol attenuates microglia-mediated neuroinflammation and ischemic brain injuries through Akt-mTOR-STAT3 signaling pathway. *Eur J Pharmacol*. 2020;883:173294. https://doi.org/10.1016/j.ejphar.2020.173294.
14 Zhang W, Tian T, Gong SX, et al. Microglia-associated neuroinflammation is a potential therapeutic target for ischemic stroke. *Neural Regen Res*. 2021; 16(1):6-11. https://doi.org/10.4103/1673-5374.286954.
15 Wang X, Yin H, Fan L, et al. Shionone alleviates NLRP3 inflammasome mediated pyroptosis in interstitial cystitis injury. *Int Immunopharmacol*. 2021;90:107132. https://doi.org/10.1016/j.intimp.2020.107132.
16 Song Y, Wu Q, Jiang H, et al. The effect of shionone on sepsis-induced acute lung injury by the ECM1/STAT5/NF-κB pathway. *Front Pharmacol*. 2021;12: 764247. https://doi.org/10.3389/fphar.2021.764247.
17 Lin L, Desai R, Wang X, et al. Characteristics of primary rat microglia isolated from mixed cultures using two different methods. *J Neuroinflammation*. 2017;14(1):101. https://doi.org/10.1186/s12974-017-0877-7.
18 Sert NPD, Hurst V, Ahluwalia A, et al. The ARRIVE guidelines 2.0: updated guidelines for reporting animal research. *BMJ Open Sci*. 2020;4(1):e100115. https://doi.org/10.1111/bph.15193.
19 Shiotsuki H, Yoshimi K, Shimo Y, et al. A rotarod test for evaluation of motor skill learning. *J Neurosci Methods*. 2010;189(2):180-185. https://doi.org/10.1016/j.jneumeth.2010.03.026.
20 Gharbawie OA, Auer RN, Whishaw IQ. Subcortical middle cerebral artery ischemia abolishes the digit flexion and closing used for grasping in rat skilled reaching. *Neuroscience*. 2006;137(4):1107-1118. https://doi.org/10.1016/j.neuroscience.2005.10.043.
21 Wang R, Wang H, Liu Y, et al. Optimized mouse model of embolic MCAO: from cerebral blood flow to neurological outcomes. *J Cereb Blood Flow Metab*. 2022;42(3):495-509. https://doi.org/10.1177/0271678X20917625.
22 Ge JW, Deng SJ, Xue ZW, et al. Imperatorin inhibits mitogen-activated protein kinase and nuclear factor κB signaling pathways and alleviates neuroinflammation in ischemic stroke. *CNS Neurosci Ther*. 2022;28(1):116-125. https://doi.org/10.1111/cns.13748.
23 Liu PY, Zhang Z, Liu Y, et al. TMEM16A inhibition preserves blood-brain barrier integrity after ischemic stroke. *Front Cell Neurosci*. 2019;13:360. https://doi.org/10.3389/fncel.2019.00360.
24 Boyko M, Ohayon S, Goldsmith T, et al. Morphological and neuro-behavioral parallels in the rat model of stroke. *Behav Brain Res*. 2011;223(1):17-23. https://doi.org/10.1016/j.bbr.2011.03.019.
25 Li Z, Bishop N, Chan SL, et al. Effect of TTC treatment on immunohistochemical quantification of collagen IV in rat brains after stroke. *Transl Stroke Res*. 2018;9(5):499-505. https://doi.org/10.1007/s12975-017-0604-9.
26 Liu DY, Huang HZ, Li K, et al. EPAC2 knockout causes abnormal tau pathology through calpain-mediated CDK5 activation. *Adv Neurol*. 2022;1(1): 1-12. https://doi.org/10.36922/an.v1i1.8.
27 Wu G, McBride DW and Zhang JH. Axl activation attenuates neuroinflammation by inhibiting the TLR/TRAF/NF-κB pathway after MCAO in rats. *Neurobiol Dis*. 2018;110:59-67. https://doi.org/10.1016/j.nbd.2017.11.009.
28 Wang Y, Ge X, Yu S, et al. Achyranthes bidentata polypeptide alleviates neurotoxicity of lipopolysaccharide-activated microglia *via* PI3K/Akt dependent NOX2/ROS pathway. *Ann Trans Med*. 2021;9(20):1522-1522. https://doi.org/10.21037/atm-21-4027.
29 Spittau B, Dokalis N, Prinz M. The role of TGF-β signaling in microglia maturation and activation. *Trends Immunol*. 2020;41(9):836-848. https://doi.org/10.1016/j.it.2020.07.003.
30 Subhramanyam CS, Wang C, Hu Q, et al. Microglia-mediated neuroinflammation in neurodegenerative diseases. *Semin Cell Dev Biol*. 2019;94:112-120. https://doi.org/10.1016/j.semcdb.2019.05.004.
31 Hendrickx DAE, van Eden CG, Schuurman KG, et al. Staining of HLA-DR, Iba1 and CD68 in human microglia reveals partially overlapping expression depending on cellular morphology and pathology. *J Neuroimmunol*. 2017;309: 12-22. https://doi.org/10.1016/j.jneuroim.2017.04.007.
32 Ma Y, Wang J, Wang Y, et al. The biphasic function of microglia in ischemic stroke. *Prog Neurobiol*. 2017;157:247-272. https://doi.org/10.1016/j.pneurobio.2016.01.005.
33 Barksby HE, Lea SR, Preshaw PM, et al. The expanding family of interleukin-1 cytokines and their role in destructive inflammatory disorders. *Clin Exp Immunol*. 2007;149(2):217-225. https://doi.org/10.1111/j.1365-2249.2007.03441.x.
34 Liberale L, Bonetti NR, Puspitasari YM, et al. TNF-α antagonism rescues the effect of ageing on stroke: perspectives for targeting inflamm-ageing. *Eur J Clin Invest*. 2021;51(11):e13600. https://doi.org/10.1111/eci.13600.
35 Lin SY, Wang YY, Chang CY, et al. TNF-α receptor inhibitor alleviates metabolic and inflammatory changes in a rat model of ischemic stroke. *Antioxidants (Basel)*. 2021;10(6):851. https://doi.org/10.3390/antiox10060851.
36 Li T, Xu T, Zhao J, et al. Depletion of iNOS-positive inflammatory cells decelerates neuronal degeneration and alleviates cerebral ischemic damage by suppressing the inflammatory response. *Free Radic Biol Med*. 2022;181: 209-220. https://doi.org/10.1016/j.freeradbiomed.2022.02.008.
37 Louveau A, Nerriere-Daguin V, Vanhove B, et al. Targeting the CD80/CD86 costimulatory pathway with CTLA4-Ig directs microglia toward a repair phenotype and promotes axonal outgrowth. *Glia*. 2015;63(12):2298-2312. https://doi.org/10.1002/glia.22894.
38 Tang JY, Cheng YB, Chuang YT, et al. Oxidative stress and AKT-associated angiogenesis in a zebrafish model and its potential application for withanolides. *Cells*. 2022;11(6):961. https://doi.org/10.3390/cells11060961.
39 Hou Y, Wang K, Wan W, et al. Resveratrol provides neuroprotection by regulating the JAK2/STAT3/PI3K/AKT/mTOR pathway after stroke in rats. *Genes Dis*. 2018;5(3):245-255. https://doi.org/10.1016/j.gendis.2018.06.001.
40 Yu M, Xue H, Wang Y, et al. miR-345 inhibits tumor metastasis and EMT by targeting IRF1-mediated mTOR/STAT3/AKT pathway in hepatocellular carcinoma. *Int J Oncol*. 2017;50(3):975-983. https://doi.org/10.3892/ijo.2017.3852.